Astron. Astrophys. 348, 594–599 (1999)

ASTRONOMY AND ASTROPHYSICS

Interstellar extinction by porous grains

D.B. Vaidya[1] **and Ranjan Gupta**[2]

[1] Department of Physics, Gujarat College, Ahmedabad 380006, India
[2] IUCAA, Post Bag 4, Ganeshkhind, Pune 411007, India

Received 7 September 1998 / Accepted 23 April 1999

Abstract. Interstellar extinction curve E(λ-V)/E(B-V) vs $1/\lambda$ is evaluated in the spectral range $3.4\,\mu$m and $0.1\,\mu$m using the extinction efficiencies of the porous silicate and graphite grains. The extinction efficiencies of the porous silicate and graphite grains are computed using the discrete dipole approximation (DDA). The model curves are compared with the average observed interstellar extinction curve. Further, we investigate the effect of porosity on the extinction in the UV in details and show that the inhomogeneity (porosity, structure) within the grains can produce shift in the central wavelength of the extinction peak in the UV, as well as variation in its width. The albedo for the porous grains in the UV and the visible spectral range is also computed and it is found to be consistent with the observations.

Key words: ISM: dust, extinction

1. Introduction

It is highly unlikely that the interstellar grains have regular shapes (i.e. spherical, cylindrical or spheroidal) or that they are homogeneous in composition and structure. The collected interplanetary particles are highly porous and consist of loosely aggregated collections of sub-grains (Brownlee, 1987). Mathis & Whiffen (1989), Henning & Stognienko (1993), Wolff et al., (1994) and Bazell & Dwek (1990) have considered that interstellar grains too have this morphology and composition. Recently, in order to overcome the 'interstellar carbon crisis' (or the abundance constraints) Mathis (1996) and Dwek (1997) have proposed a composite fluffy dust model. The optical properties of these porous and fluffy particles should be quite different from those of solid homogeneous particles. Unfortunately, it is not yet possible to rigorously treat the absorption and scattering of light by porous (inhomogeneous) or irregularly shaped particles. In general, there are two approaches to calculate optical properties of the inhomogeneous (porous) particles. One approach is to use the finite element method. e.g. Discrete Dipole Approximation (DDA). The second approach is the application of the effective medium theories (EMT's). In EMT the inhomogeneous particle is replaced by a homogeneous one with some averaged 'effective' dielectric function (for discussion on EMT see e.g. Bohren & Huffman, 1983). The effects related to the fluctuations of the dielectric function within the inhomogeneous structures such as surface roughness and special distributions of the components can not be treated by the averaging approach of the EMT's. The discrete dipole approximation (DDA) allows the consideration of irregular shape effects and special distributions of the components in the particles (Wolff et al., 1994; Wolff et al., 1998).

In our earlier paper (Vaidya & Gupta 1997, hereafter Paper I) using DDA we had obtained the extinction efficiencies of the porous silicate and graphite grains and we had evaluated the interstellar extinction curve between $0.55\,\mu$m and $0.20\,\mu$m. These results clearly showed that the extinction properties of the grains are modified if the grains are porous. This motivated us to study the extinction properties of the porous silicate and graphite grains in the wavelength range between $0.55\,\mu$m to $3.4\,\mu$m in the infrared and from $0.20\,\mu$m to $0.10\,\mu$m in the ultraviolet region and to evaluate the interstellar extinction curve (i.e. E(λ-V)/E(B-V) vs $1/\lambda$) in the entire wavelength range of 0.10 to $3.4\,\mu$m. We have also evaluated the albedo, i.e. the ratio of $\mathrm{Q_{sca}}/\mathrm{Q_{ext}}$ for the porous grains in the UV and the optical region.

In Sect. 2 we give the validity criteria for the DDA and the porous grain models. In Sect. 3 we present the results of our computations and discuss these results. The main conclusions of our study are given in Sect. 4.

2. Discrete Dipole Approximation (DDA) and porous grain models

Validity Criteria for Discrete Dipole Approximation:

The discrete dipole approximation (DDA) method is described by Purcell & Pennypacker (1973) and Draine (1988). The DDA replaces the solid particle by an array of N point dipoles. When a grain is exposed to an electromagnetic wave, each dipole is under the radiation field of the incident wave as well as the fields due to all other dipoles. There are two validity criteria for DDA (Draine & Flatau, 1994 and Wolff et al., 1994); viz. (i) $|m|kd \leq 1$ where m is the complex refractive index, $k = \pi/\lambda$ is the wave number, and d is the lattice dispersion spacing and (ii) d should be small enough (N should be sufficiently large) to describe the shape of the particle satisfactorily. We have used the DDA program 'DDSCAT.4c' (Draine & Flatau, 1995) to

Send offprint requests to: Ranjan Gupta (rag@iucaa.ernet.in)

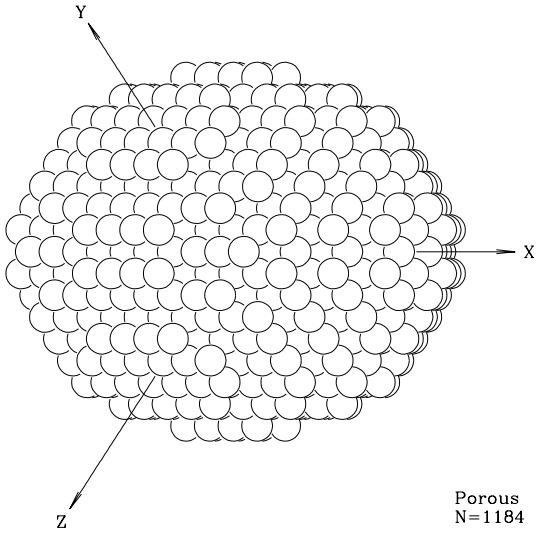

Fig. 1. A model of the porous dust grain with N = 1184 dipoles

generate the porous grains. In this program it is assumed that the dipoles are located on a cubic lattice. Initially we assume a large number of dipoles Nx, Ny, Nz along the axis x, y, z for the spheroidal target grain. This would result in a certain number of N dipoles in the solid grain (e.g. N = 4088 in the present case). Then we reduce Nx, Ny, Nz to generate the porous grains. These dipoles are reduced such that the shape of the grain does not change. The assumed shape of the grain is a prolate spheroid with axial ratio of 1.3. If the semi-major axis and semi-minor axis of the prolate spheroids are denoted by $x/2$ and $y/2$ respectively then $a^3 = (x/2) * (y/2)^2$; where a is the radius of a sphere whose volume is the same as that of a spheroid.

The porosity P is defined as $\mathrm{P} = 1 - \mathrm{V_{solid}}/\mathrm{V_{total}}$; where $\mathrm{V_{solid}}$ is the volume of the solid material inside the grain and $\mathrm{V_{total}}$ is the total volume of the grain (Greenberg, 1990; Hage & Greenberg, 1990). The porosity P of the grain varies between $0 < \mathrm{P} < 1$. Accordingly, using DDSCAT.4c the porous grain models with the number of dipoles N = 4088, 1184 and 152 are generated (Vaidya & Desai, 1996 and Paper I). These levels of porosities are selected to maintain the spheroidal shape of the grain i.e. axial ratio of 1.3).

As an illustrative example we show in Fig. 1 the porous grain model with N = 1184. This figure is produced by using the 'calltarget' and 'dtarget' programs (Draine & Flatau, 1995).

Tables 1 & 2 show the maximum radius (a_{max}) of the grain that satisfies the validity criteria for DDA (viz. $mkd = 1$) at several wavelengths for N = 4088, 1184 and 152 for silicates and graphite respectively. The complex refractive indices m for silicates and graphite are obtained from Draine (1985, 1987). In the case of graphite, results for both the dielectric functions i.e. parallel (Ell) and perpendicular (Elr) are shown.

It is seen from the Table 1 & 2 that in the UV region the DDA is valid for grain sizes of about $0.1\,\mu$ for N = 1184 and about $0.2\,\mu$ for N = 4088 whereas in the IR it is valid for larger grain sizes, between $0.2\,\mu$ and $2.0\,\mu$ for N = 1184 and between $0.3\,\mu$ and $3.0\,\mu$ for N = 4088. Porous grains with N = 152 need

Table 1. Validity Criteria for silicate Grains

Wavelength (μm)	Silicate N = 152 $a_{max}(\mu)$	Silicate N = 1184 $a_{max}(\mu)$	Silicate N = 4088 $a_{max}(\mu)$
0.1000	0.030	0.06	0.09
0.1500	0.030	0.07	0.10
0.2000	0.055	0.11	0.17
0.3000	0.090	0.19	0.25
0.5500	0.170	0.35	0.50
0.7000	0.215	0.42	0.63
1.0000	0.308	0.64	0.92
2.2000	0.678	1.34	2.03
3.4000	1.000	2.08	3.12

to be very small (less than $0.1\,\mu$) in order to satisfy the DDA validity criteria in the UV. In Paper I we had given a table as well as two figures showing the range of applicability of DDA in the spectral range, $0.20\,\mu$m–$0.55\,\mu$m, for the porous silicate and graphite (Elr) grains.

Using DDA, Wolff et al., (1994) have investigated the effects of porosity on electromagnetic scattering and have compared their results with those obtained using the effective medium theory (EMT). Vaidya & Desai (1996) have used DDA to study the scattering properties of porous grains. They have used the porous grain model to explain the low density and low albedo observed in the dust coma of the comet Halley. DDA has also been utilized to study composite particles and to determine the limits of EMT (Bazell & Dwek, 1990; Perrin & Lamy, 1990; Ossenkopf, 1991; Stognienko et al., 1995 and Wolff et al., 1993).

3. Results and discussion

In Paper I, we had presented results for the extinction by the porous silicate and graphite grains in the wavelength region from $0.20\,\mu$m to $0.55\,\mu$m. The enhancement in the extinction for porous grains was clearly indicated at certain wavelengths and for some wavelengths it deviated from that obtained for the solid grains. This motivated us to study the effect of porosity on the extinction for the silicate and graphite grains in the near infrared wavelengths between $0.70\,\mu$m and $3.4\,\mu$m as well as in the ultraviolet region between $0.20\,\mu$m and $0.10\,\mu$m. In this paper we present the results for the entire spectral range from $3.4\,\mu$m to $0.10\,\mu$m; i.e. 22 wavelengths. The prolate spheroidal grains are assumed to be randomly oriented.

Silicates: Fig. 2 shows the plots of the extinction efficiency $\mathrm{Q_{ext}}$ vs $1/\lambda$ for the porous (N = 152,1184,4088) silicate grains in the wavelength range of $0.10\,\mu$m–$3.4\,\mu$m for the grain size (i)$a = 0.01\,\mu$ (ii)$a = 0.05\,\mu$ (iii)$a = 0.10\,\mu$ and (iv)$a = 0.25\,\mu$.

These plots show that for small grain sizes (i.e. $0.01\,\mu$ and $0.05\,\mu$) there is not much variation in the extinction with the porosity whereas for larger grain sizes ($a = 0.10\,\mu$ and $0.25\,\mu$) the extinction is modified considerably especially in the visible and the UV region. For these large grain sizes each porous grain model is valid upto a certain wavelength (see Table 1) beyond

Table 2. Validity criteria for graphite grains

Wavelength (μm)	Grap(Ell) N = 152 $a_{max}(\mu)$	Grap(Ell) N = 1184 $a_{max}(\mu)$	Grap(Ell) N = 4088 $a_{max}(\mu)$	Grap(Elr) N = 152 $a_{max}(\mu)$	Grap(Elr) N = 1184 $a_{max}(\mu)$	Grap(Elr) N = 4088 $a_{max}(\mu)$
0.1000	0.03	0.05	0.07	0.020	0.04	0.07
0.1500	0.04	0.08	0.12	0.060	0.13	0.20
0.2000	0.06	0.13	0.20	0.080	0.17	0.25
0.3000	0.08	0.15	0.25	0.050	0.10	0.15
0.5500	0.10	0.21	0.33	0.091	0.19	0.27
0.7000	0.16	0.33	0.50	0.111	0.22	0.33
1.0000	0.24	0.48	0.70	0.142	0.28	0.72
2.2000	0.54	1.07	1.62	0.242	0.48	0.72
3.4000	0.84	1.66	2.52	0.322	0.63	0.96

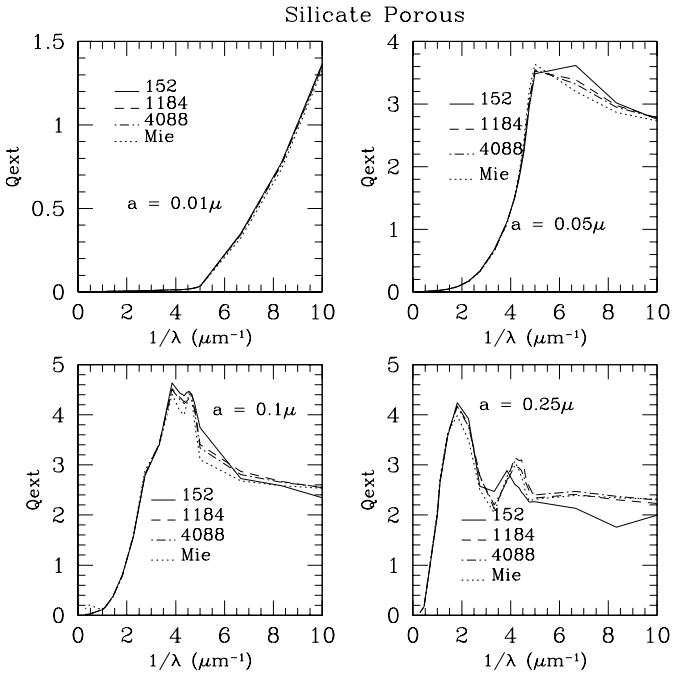

Fig. 2. Extinction efficiencies (Q_{ext}) for porous Silicate grains.

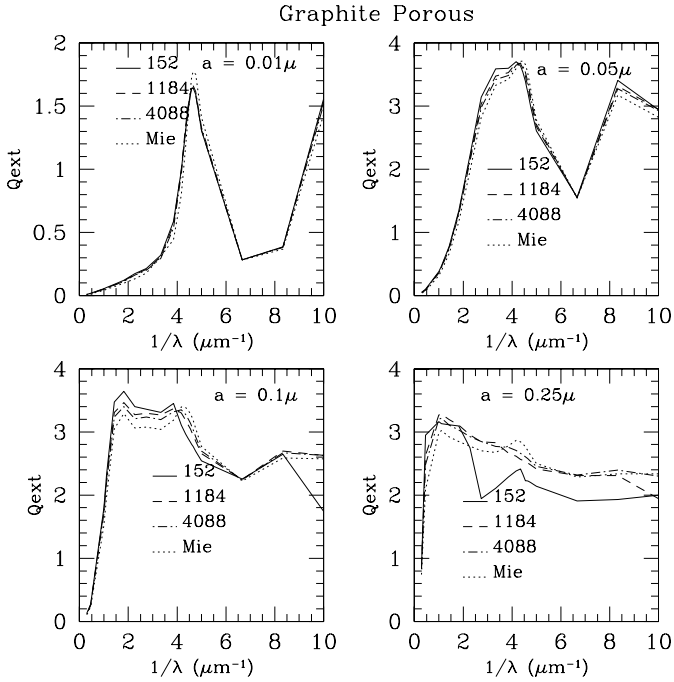

Fig. 3. Extinction efficiencies (Q_{ext}) for porous Graphite grains.

this wavelength the extinction curve would show irregularity; e.g. especially N = 152 in the UV spectral range; i.e. $0.30\,\mu$m–$0.10\,\mu$m. Fig. 2 also shows Q_{ext} curves for solid spherical grains obtained using Mie theory.

Graphites: Fig. 3 shows plots of Q_{ext} vs $1/\lambda$ for the porous graphite grains with (i)$a = 0.01\,\mu$ (ii)$a = 0.05\,\mu$ (iii)$a = 0.1\,\mu$ and (iv)$a = 0.25\,\mu$. Except for the curves with a very small grain size, i.e. (i)$a = 0.01\,\mu$, all the other curves i.e. for $a = 0.05, 0.1$ and $0.25\,\mu$ show the variation in the extinction with the porosity. As mentioned earlier in the case of silicates, for large grain sizes; i.e. $a = 0.1\,\mu$ and $a = 0.25\,\mu$; each porous grain model will be valid upto a certain wavelength (check Table 2) and beyond that wavelength the extinction curves for that model would start showing irregularities (e.g. N = 152 in the UV spectral range). These curves also show a shift in the central wavelength of the extinction peak, as well as the variation in the width of the peak, as the porosity increases.

In order to emphasize these aspects we show in Fig. 4, the extinction efficiency Q_{ext} for the porous graphite grains for $a = 0.05\,\mu$ in the wavelength region $0.2\,\mu$m–$0.30\,\mu$m. This plot shows the shift in the absorption peak; from $4.5\,\mu\mathrm{m}^{-1}$ for solid Mie curve to $4.1\,\mu\mathrm{m}^{-1}$ for porous grains with N = 152. It also shows the variation in the width of the 'bump'; i.e. it broadens as the porosity increases. These results on the porous graphite grains show that the inhomogeneity within the grains can produce shift in the central wavelength of the extinction bump as well as the variation the width of the bump. For small graphite grains $a = 0.005\,\mu$, Perrin & Sivan (1990) had found that the width of the extinction bump was modified by porosity but the maximum of the bump did not shift with porosity. Draine & Malhotra (1993) have found the shift in the central wavelength

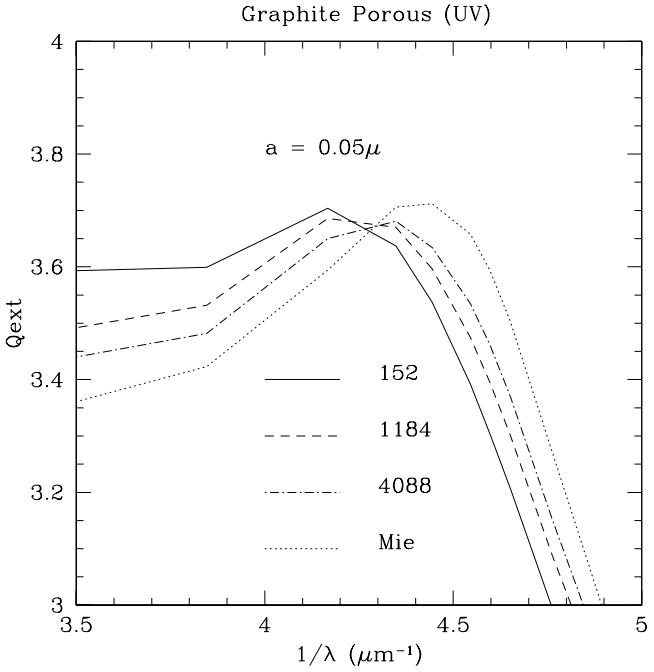

Fig. 4. Extinction efficiencies (Q_{ext}) for porous Graphite grains in the UV region for grain size $0.05\,\mu$.

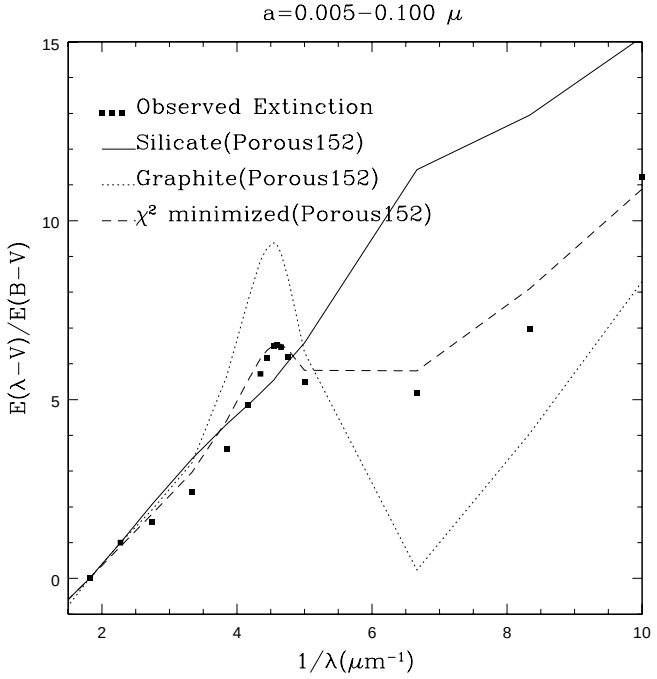

Fig. 5. Comparison of the observed interstellar extinction curve with the best fit model combination curve of porous silicate and graphite grains with the number of dipoles N = 152.

of the bump in the coagulated graphite grains, but they did not find any appreciable change in the profile width.

Interstellar Extinction Curve: The interstellar extinction curve (i.e. the variation of extinction with wavelength) is usually expressed by the ratio E(λ-V)/E(B-V) vs $1/\lambda$ and the ratio R of total to selective extinction is expressed as $\mathrm{R} = \mathrm{A_v}/\mathrm{E(B-V)}$. The average observed value of R is 3.1 (e.g. Savage & Mathis, 1979).

We use the extinction efficiencies of the porous silicate and graphite grains and the power law grain size distribution (i.e. $\mathrm{n(a)} \sim \mathrm{a}^{-3.5}$, see e.g. Mathis et al., 1977) to reproduce the interstellar curve.

The average observed interstellar extinction curve (Savage & Mathis, 1979) is then compared with the model curve formed from a χ^2 minimized and best fit linear combination of porous silicate and graphite grains in the following way:

The two model interstellar extinction curves for silicate and graphite porous grains are linearly combined as p times silicate and q times graphite to render a net curve for comparison with the observed curve. By varying p and q individually from 0.1 to 1.0 in steps of 0.1, a set of 20 curves are generated and the comparison with the observed curve gives a set of reduced $\tilde{\chi^2}_j$values. The combination of p and q which gives a minimum $\tilde{\chi^2}_j$ value in this set is chosen and such combinations and corresponding minimum $\tilde{\chi^2}_j$ values are shown in the Table 4.

The set of reduced $\tilde{\chi^2}_j$ values is defined as (Bevington, 1969):

$$\tilde{\chi^2}_j = \frac{\sum_{i=1}^{n}(S_i^j - T_i^k)^2}{pp} \qquad (1)$$

where pp is the degrees of freedom, $S_i^j(\lambda_i)$ is the j^{th} model curve for the corresponding p and q linear combination of silicate and graphite porous grains and $T_i^k(\lambda_i)$ is for the observed curve, λ_i are the wavelength points with $i = 1, n$ for $n = 22$ points of the extinction curves.

Figs. 5, 6 and 7 show the best fit interstellar extinction curves for the porous grain models N = 152, N = 1184 and N = 4088 respectively. Table 4 shows the best fit parameters p, q and χ^2 for three size distributions that we have used for these curves. These values of p and q indicate the proportions of silicate and graphite components required to fit the observed extinction curve. It is seen that in most of the cases, the combination of 50% silicate and 40% graphite fit the observed extinction curve best.

It is to be noted here that for the grain models with N = 152 (Fig. 5) we have considered small grain sizes that satisfy the DDA validity criteria. As a result models with N = 152 do not fit well in the ir and the visible spectral range but they fit reasonably well in the bump region (i.e. $0.23\,\mu\mathrm{m}$–$0.20\,\mu\mathrm{m}$). Grain Models with N = 1184 and N = 4088 with larger grain sizes fit better with the observed curve (Figs. 6 & 7).

Extinction in the UV and the '2175' feature: Despite continuing research over the last 30 years, the identification of the 2175 Å feature remains controversial. The most widely accepted explanation of the 2175 Å bump has been the extinction by small graphite interstellar grains (e.g. Hoyle and Wickramasinghe, 1962; Mathis et al., 1977 and Draine, 1988). However, as indicated earlier, the structure of the grains also plays an important role in the interstellar extinction. Using the extinction efficien-

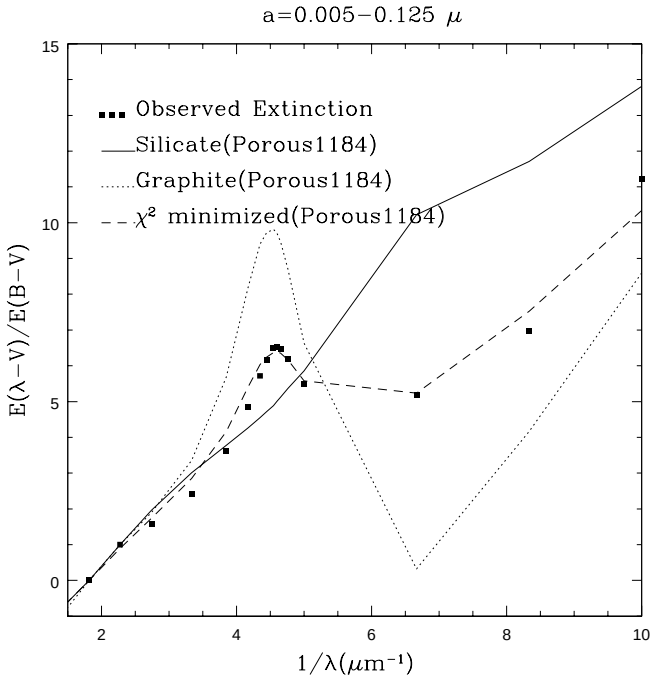

Fig. 6. Comparison of the observed interstellar extinction curve with the best fit model combination curve of porous silicate and graphite grains with N = 1184.

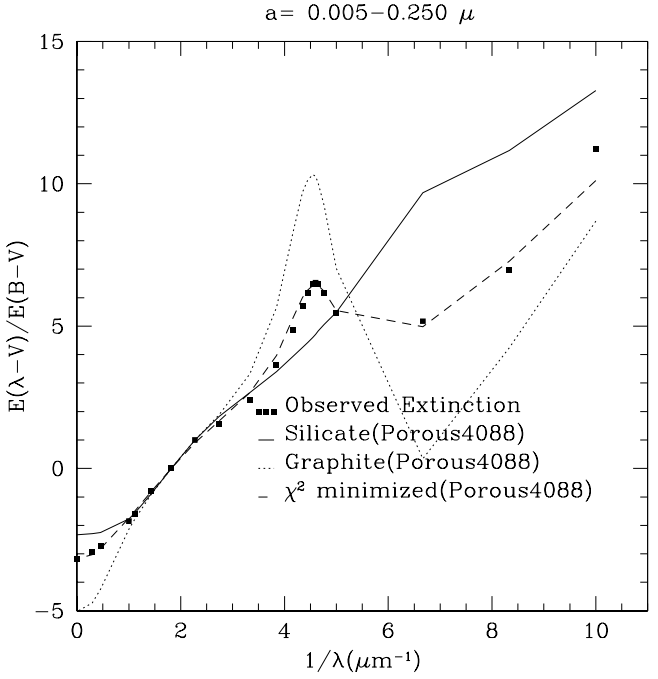

Fig. 7. Comparison of the observed interstellar extinction curve with the best fit model combination curve of porous silicate and graphite grains with N = 4088.

cies for small ($0.001\,\mu$–$0.100\,\mu$) graphite and silicate porous grains in the wavelength region $0.3650\,\mu$m–$0.20\,\mu$m we evaluate the interstellar extinction curve. Fig. 8 shows the interstellar extinction curve in the 'bump' region i.e. $0.3650\,\mu$m–$0.20\,\mu$m for the porous grains with N = 152.

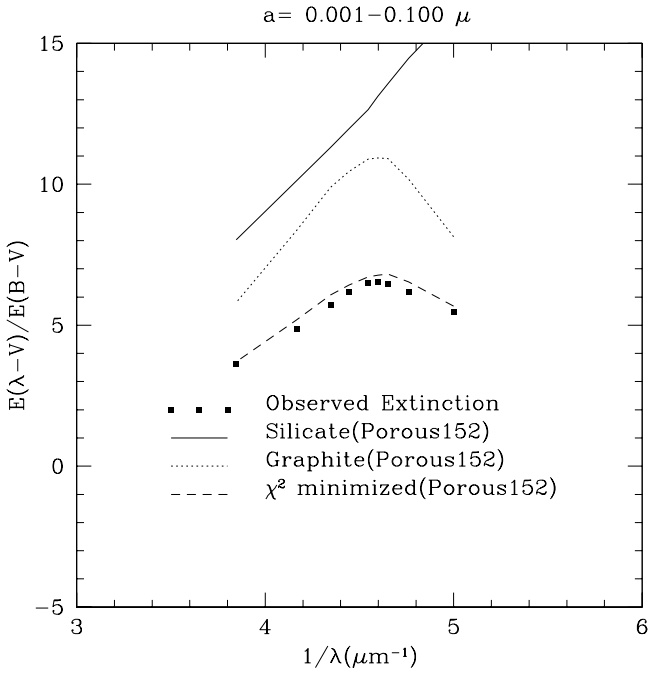

Fig. 8. Comparison of the observed interstellar extinction curve in the 'bump' region with the best fit model combination curve of porous silicate and graphite grains with N = 152.

Table 3. Best fit values of p, q and minimized χ^2 for porous grains of sizes 0.005–$0.250\,\mu$, 0.005–$0.125\,\mu$ and 0.005–$0.100\,\mu$ and number of dipoles N = 152,1184 and 4088

Parameters	0.005–0.250	0.005–0.125	0.005–0.100
No. of dipoles N = 152			
p	0.6	0.5	0.5
q	0.4	0.4	0.4
χ^2	0.1639	0.1509	0.2371
No. of dipoles N = 1184			
p	0.5	0.5	0.5
q	0.4	0.4	0.4
χ^2	0.1083	0.1344	0.2858
No. of dipoles N = 4088			
p	0.5	0.5	0.4
q	0.4	0.4	0.4
χ^2	0.094	0.1393	0.2774

These results show that small porous grains with about 60%–70% porosity fit the observed extinction in the bump region reasonably well.

Albedo: In Fig. 9, we show the variation of the albedo $A = Q_{sca}/Q_{ext}$ for the porous grain model with N = 1184 in the optical and the UV spectral range.

The visual albedo of the porous grain model is about 0.6, which is in agreement with the value suggested by Witt (1989). The albedo predicted by the composite fluffy dust (CFD) model is lower, about 0.5 (Mathis, 1996 and Dwek, 1997). The low albedo of the CFD model was found to be the cause of the excess

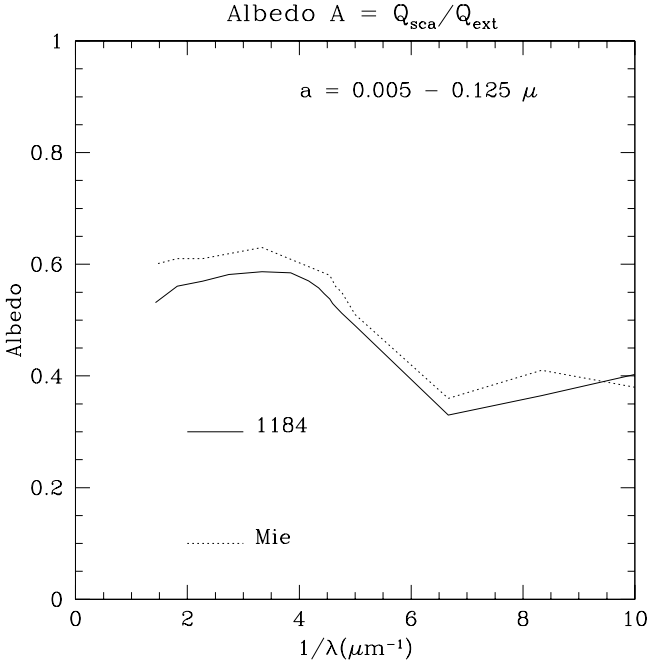

Fig. 9. Curves showing the albedo variation in the optical and the UV range.

far infrared emission of that observed with the COBE/DIRBE and FIRAS instruments from the diffuse interstellar medium (Dwek, 1997). This would mean that with the higher albedo the porous grain model which we have considered here would re-emit less radiation in the far infrared region than that is emitted by the CFD model and would fit the COBE data better.

4. Conclusions

We have studied the effects of porosity on the extinction of the silicate and graphite grains in the spectral range of $3.4\,\mu\mathrm{m}$–$0.10\,\mu\mathrm{m}$. For these calculations the discrete dipole approximation is used because it takes into consideration the inhomogeneous structure (porosity, surface roughness) within the grain (Wolff et al., 1994 & 1998). The extinction curves for the porous graphite grains show the shift in the central wavelength of the extinction peak as well as variation in the width of the peak, with the porosity. These results on the porous grains indicate that the structure of the grains plays an important role in the interstellar extinction and needs to be studied in more details. We found that the porous grain models reproduce the average observed extinction reasonably well. The visual albedo for the porous grain model is about 0.6 which is found to be consistent with the observations. The application of DDA (or the validity criteria for DDA) however poses a computational challenge particularly for large values of the size parameter $\mathrm{x}(=2\pi\mathrm{a}/\lambda)$ and the refractive index $|\mathrm{m}|$, since greater number of dipoles N are required; which would in turn require large computer memory and considerable cpu time. The effective medium theory with Mie-type series solutions, may still play an important role in deriving the properties of interstellar dust (Wolff et al., 1998). However, before applying the EMT, the accuracy and the range of applicability of several mixing rules need to be determined (Chylek et al., 1988 and Ossenkopf, 1991). It would be very useful to compare the DDA scattering properties for porous grains (with a range of porosity) with those computed by the EMT/series solution technique in order to examine the applicability of several mixing rules. A synthetic approach combining the laboratory data on the porous and fluffy particles (Gustafson, 1996 and Zerull et al., 1993) with the theoretical calculations would also help greatly to interpret the observed interstellar extinction and polarization.

Acknowledgements. We thank Prof. B. T. Draine for providing the DDSCAT.4c and DTARGET programs. We thank the referee for his constructive suggestions which greatly improved the presentation of the paper. DBV thanks Physical Research Laboratory, Ahmedabad, and IUCAA, Pune for providing the computational and other facilities.

References

Bazell D., Dwek E., 1990, ApJ, 360, 142
Bevington, P.R., 1969, Data Reduction and Error Analysis for the Physical Sciences (New York: McGraw-Hill), Chapter 1–4
Bohren C.F., Huffman D.R., 1983, Absorption and Scattering of Light by Small Particles, John Wiley, New York
Brownlee D., 1987, in Interstellar Processes eds. Hollenbach & Thomson H., Dordrecht, Reidel, 513
Chylek P., Srivastava V., Pinnick R.G., Wang R.T., 1988, Appl. Opt., 27, 2396
Draine B.T., 1985, ApJ(supp), 57, 587
Draine B.T., 1987, Princeton Observatory Reprint No. 213
Draine B.T., 1988, Ap.J., 333, 848
Draine B.T., Flatau P.J., 1994, J.O.S.A., A, 11, 1491
Draine B.T., Flatau P.J., 1995, User Notes for DDSCAT.4c
Draine B.T., Malhotra S., 1993, ApJ, 414, 632
Dwek E., 1997, ApJ, 484, 779
Greenberg J.M., 1990,in Comet Halley, Vol.2., Ed. Mason J., 105
Gustafson B.A.S., 1996, J. Quant. Spect. Rad. Transfer, 55;5, 663
Hage J., Greenberg J.M. 1990 ApJ, 361, 251
Henning Th., Stognienko R., 1994, A&A, 280, 609
Hoyle F., Wickramasinghe N.C., 1962, MNRAS, 124, 417
Mathis J.S., 1996, ApJ, 472, 643
Mathis J.S., 1990, Ann. Rev. A&A, 17, 73
Mathis J.S., Rumpl W., Nordsieck K.H., 1977, ApJ, 217, 425
Mathis J.S., Whiffen G., 1989, ApJ, 341, 808
Ossenkopf V., 1991, A&A, 251, 210
Perrin J.M., Lamy P.L., 1990, ApJ, 364, 146
Perrin J.M., Sivan J.-P., 1990, A&A, 228, 238
Purcell E.M., Pennypacker C.R., 1973, ApJ, 186, 705
Savage B.D., Mathis J.S., 1979, Ann. Rev. A&A, 17, 73
Stognienko R., Henning Th., Ossenkopf V., 1995, ApJ, 296, 797
Vaidya D.B., Desai J.N., 1996, A.S.P. Conf. Ser., 104, 433
Vaidya D.B., Gupta R., 1997, A&A, 328, 634 (Paper I)
Witt A.N., 1989, in Interstellar Dust, eds. Allamandola & A.G.G.M. Tielens, Dodrecht, Kluwer, 87
Wolff M.J., Clayton G.C., Meade M.R., 1993, ApJ, 403, 722
Wolff M.J., Clayton G.C., Martin P.G., Sculte-Ladback R.E., 1994, ApJ, 423, 412
Wolff M.J., Gibson S.J., Clayton G.C., 1998, Preprint
Zerull R.H., Gustafson B.A.S., Schulz K., Theile-Corbach E., 1993, Appld. Opt., 34:21, 4088